Los Alamos
NATIONAL LABORATORY
EST. 1943

LA-UR-21-28773
Approved for public release; distribution is unlimited.

Title: Radiation Hydrodynamics in the Lagrangian Application Project's LUMOS code.

Author(s): Thompson, Kelly Glen
Wollaeger, Ryan Thomas
Budge, Kent Grimmett

Intended for: Report

Issued: 2021-09-03

Disclaimer:
Los Alamos National Laboratory, an affirmative action/equal opportunity employer, is operated by Triad National Security, LLC for the National Nuclear Security Administration of U.S. Department of Energy under contract 89233218CNA000001. By approving this article, the publisher recognizes that the U.S. Government retains nonexclusive, royalty-free license to publish or reproduce the published form of this contribution, or to allow others to do so, for U.S. Government purposes. Los Alamos National Laboratory requests that the publisher identify this article as work performed under the auspices of the U.S. Department of Energy. Los Alamos National Laboratory strongly supports academic freedom and a researcher's right to publish; as an institution, however, the Laboratory does not endorse the viewpoint of a publication or guarantee its technical correctness.

Los Alamos NATIONAL LABORATORY

Memorandum

Computational Physics and Methods

To: Distribution
From: Kelly Thompson, CCS-2, MS D409
Ryan Wollaeger, CCS-2, MS D409
Kent Budge, CCS-2, MS D409
Phone: 505-665-8090

Symbol: CCS-2:21-048(U)
Date: July 12, 2021

Subject: (U) Radiation Hydrodynamics in the Lagrangian Application Project's LUMOS code.

Executive Summary

Starting in 2019, the Lagrangian Applications Project (LAP) and the Transport Project set out to develop a new ALE/Lagrangian radiation-hydrodynamics (RH) capability in a new code product named LUMOS. This work was done under the guidance of the Advanced Simulation and Computing (ASC) program with the goal of producing software capable of leveraging the high-order thermal radiative transfer (TRT) solvers provided by the Jayenne and Capsaicin software projects. This capability supplements the existing gray diffusion solver that is currently available in LAP's FLAG code [1, 2, 3] for RH.

The remainder of this memo describes the coupling of the radiation and hydrodynamics solvers within LAP's LUMOS code. Initially delivered in 2020 as part of an L2 milestone [4], this capability continues to mature in FY21 with more efficient and robust algorithms, new support for ALE, and support for mixed materials per cell. Today, LUMOS is provided as a standard end-user product in the suite of LAP tools provided in each release cycle. Code access can be requested at https://asc.lanl.gov.

Introduction

Accurate modeling of radiation-hydrodynamics problems is important for many high-energy density physics (HEDP) applications such as Inertial Confinement Fusion (ICF), astrophysical problems and radiation flow experiments. In such applications, the system generally consists of both optically thick and thin media. In the thin limit, the diffusion approximation for TRT breaks down, exhibiting unphysical information propagation speeds, inability to capture anisotropy, and smearing of the solution. In such problems, it is desirable to employ a high order TRT solver like the Implicit Monte Carlo (IMC) or Discrete Ordinates (S_N) methods.

Building on the work done by Park [5], we have identified many RH codes that leverage high-order radiation transport algorithms. A selection of these codes are provided in Table 1 on the next page. When reviewing these efforts, we find that astrophysical application codes tend to use Eulerian hydro schemes, while ICF application codes often use Arbitrary Lagrangian Eulerian (ALE) hydro schemes (LANL's xRAGE code [6], used by many ICF applications, is an exception). All of the codes listed in this table use either S_N, Monte Carlo (MC) or Implicit Monte Carlo (IMC) techniques for radiation transport.

Recent work by LAP and the Transport Project in their development of a new radiation-hydrodynamic simulation capability was highlighted in [7]. In the following section, we discuss, in detail, the Lagrangian radiation-hydrodynamics algorithms and operator split implemented in the LUMOS code. We also highlight the operator-split used for each time step and the data that must passed between the hydrodynamics code and the TRT solver.

Table 1. Existing radiation-hydrodynamics codes.

Code	Hydro method	Radiation method	Institution
Symphony [5]	Lagrangian	SN	LANL (USA)
TROLL [8]	ALE	IMC	CEA (France)
TORUS [9]	Eulerian	IMC	UK
FLASH [10]	Eulerian	IMC	University of Chicago (USA)
AREPO-MCRT [11]	Lagrangian	IMC	
BHLIGHT [12]	Eulerian MHD	MC	University of Illinois (USA)
MULTI [13, 14, 15]	Lagrangian	SN	Germany
SARA [16]	Lagrangian	SN	Spain
ZEUS-2D [17]	Eulerian	SN	University of Illinois (USA)
ATHENA [18, 19]	Eulerian	SN	University of Illinois (USA)
VULCAN [20]	Eulerian (Lagrangian + remap)	SN	Princeton University (USA)

A Brief Development of the Lagrangian Radiation Hydrodynamics Equations

Nomenclature and other useful information

The equations for thermal radiative transfer (TRT) discussed below use the following nomenclature.

$I = chvn(\vec{r}, \hat{\Omega}, \nu, t)$ the specific intensity, GJ/cm^2-ns-keV-sr, where

$n(\vec{r}, \hat{\Omega}, \nu, t)$ the mean number of photons per unit of phase space

$h = 4.135667516\text{x}10^{-19}$ keV-ns Planck's constant

$c = 29.9792458$ cm/ns speed of light

$T(\vec{r}, t), \rho(\vec{r}, t), \vec{U}(\vec{r}, t)$ the material temperature (keV), density (g/cm^3), and velocity (cm/ns)

$$B = B(\nu, T) = \frac{2T^3}{h^3c^2}\frac{(\nu/T)^3}{e^{\nu/T} - 1}$$ Planck's function for radiation emission, GJ/cm^2-ns-keV-sr (1)

$Q_m(\vec{r}, \nu, t), Q_r(\vec{r}, \nu, t)$ inhomogeneous material/photon source, GJ/ cm^3-ns-keV

$c_v(\vec{r}, T)$ heat capacity of the material, GJ/keV- cm^3

$\sigma_a(\vec{r}, \nu, T), \sigma_s(\vec{r}, \hat{\Omega}' \to \hat{\Omega}, \nu' \to \nu, t)$ the absorption and differential scattering opacities, cm^{-1} (2)

$$a = \frac{8\pi^5k^4}{15h^3c^3} = 0.01372$$ radiation constant, GJ/cm^3-keV^4 (3)

In the TRT equations, the quantities T and I are unknown; all other quantities are prescribed (but can depend on T and I). It is also convenient to express the *material energy density,* $\mathcal{E}$, and the equilibrium radiation energy density E, which are given by the relationships

$$\frac{\partial e}{\partial T}(\vec{r},t) = \frac{c_v(\vec{r},T)}{\rho}, \quad E(\vec{r},t) = aT(\vec{r},t)^4. \tag{4}$$

It is also useful to define the frequency-normalized Planck spectrum

$$b(\nu,T) \equiv \frac{B(\nu,T)}{\int_0^\infty B(\nu,T)d\nu}. \tag{5}$$

Combining equations (1), (4), and simplifying, the frequency-integrated Planck spectrum can be expressed as

$$\int_0^\infty B(\nu,T)d\nu = \frac{2\pi^4 T^4}{15h^3c^2} = \frac{caT^4}{4\pi} = \frac{cE}{4\pi}, \tag{6}$$

and the frequency-normalized Planck spectrum from equations (5) and (6) is

$$b(\nu,T) = \frac{15}{\pi^4}\frac{1}{T}\frac{(\nu/T)^3}{e^{\nu/T}-1},$$

and by definition, satisfies

$$\int_0^\infty b(\nu,T)d\nu = 1.$$

It is also useful to define the *Planck opacity* as a Planck frequency-normalized weighted opacity,

$$\sigma_P \equiv \int_0^\infty \sigma(\nu,T)b(\nu,T)d\nu.$$

From (5) and (6) we note

$$B(\nu,T) = b(\nu,T)\int_0^\infty B(\nu,T)d\nu = b(\nu,T)\frac{caT^4}{4\pi} = b(\nu,T)\frac{cE}{4\pi} \tag{7}$$

so that

$$\int_0^\infty \sigma_a B(\nu,T)d\nu = \frac{caT^4}{4\pi}\int_0^\infty \sigma_a b(\nu',T)d\nu' = \frac{caT^4}{4\pi}\sigma_{P.} \tag{8}$$

Finally, we find it useful to define a relationship between ε and E,

$$\beta(\vec{r},t) = \frac{\partial E}{\partial \mathcal{E}} = \frac{dE/dT}{d\varepsilon/dT} = \frac{4aT^3}{c_v(T)}.$$

It should also be noted that the specific intensity, *I,* is related to the radiation energy density, *E,* radiative flux, $\vec{F}$, and radiation pressure tensor, $\mathbb{P}$, by the following relationships,

$$U_r \equiv \frac{1}{c}\int_0^\infty \int_{4\pi} I d\Omega d\nu, \qquad \vec{F} \equiv \int_0^\infty \int_{4\pi} \hat{\Omega} I d\Omega d\nu, \qquad \mathbb{P} = \frac{1}{c}\int_{4\pi}\int_0^\infty \hat{\Omega}\hat{\Omega} I d\nu d\Omega. \tag{9}$$

Development of the Eulerian Radiation Hydrodynamics Equations

As carriers of electromagnetic force, photons impart momentum to matter via interaction with charged particles (e.g. free electrons or electrons bound to an atomic orbital). The cumulative effect of photon-matter interactions on the energy and momentum of a fluid is a topic of radiation hydrodynamics. More generally, radiation hydrodynamics is the study of the interaction between particles with dynamics that can be described with a transport or diffusion equation (radiation) with particles that behave hydrodynamically (fluid/material). The origin of both the transport equation and hydrodynamics equations is the Boltzmann equation. The photon transport equation is straightforward to derive from the Boltzmann equation. Following the development from the Jayenne Physics Manual [21], it can be shown that in local thermodynamic equilibrium, the photon transport equation takes the form,

$$\frac{1}{c}\frac{\partial I}{\partial t} + \hat{\Omega}\cdot\nabla I + (\sigma_s + \sigma_a)I = \int_{4\pi}\int_0^\infty \sigma_s(\nu' \to \nu, \hat{\Omega}' \to \hat{\Omega}) I' d\nu' d\Omega' + \sigma_a B, \tag{10}$$

where all of the terms are described above in the section on nomenclature. Subsequently, a diffusion equation can be obtained through a limit analysis treatment of the photon transport equation as shown in [21, 22].

The Boltzmann equation is also the source of our standard hydrodynamic equations when it is applied to massive particles that interact by two-body collisions and neglecting external long-distance interactions.

The manipulations discussed in [23, 24, 25, 26, 27] produce a Boltzmann equation that can be multiplied by $m, m\vec{v}$, and $m|\vec{v}|^2/2$, and integrating over velocity space to yield (full details are provided in [21]),

$$\begin{aligned} \frac{\partial \rho}{\partial t} + \nabla \cdot \left(\rho \vec{U}\right) &= 0, \\ \frac{\partial \left(\rho \vec{U}\right)}{\partial t} + \nabla \cdot \left(\mathbf{P} + \rho \vec{U}\vec{U}\right) &= 0, \\ \frac{\partial}{\partial t}\left(\rho e + \frac{1}{2}\rho U^2\right) + \nabla \cdot \left(\vec{Q} + \vec{U}\rho e + \frac{\vec{U}\rho U^2}{2} + \mathbf{P} \cdot \vec{U}\right) &= 0, \end{aligned} \tag{11}$$

where we have used the following nomenclature

$\rho(\vec{r}, t)$ density, g/cm^3
$\vec{U}(\vec{r}, t)$ velocity vector, cm/ns
$\boldsymbol{P}(\vec{r}, t)$ pressure tensor, g/cm-ns^2
$e(\vec{r}, t)$ material specific energy, cm^2/ns^2
$\vec{Q}$ external source, g/ns^2.

These are the hydrodynamic (Euler) equations without external sources (i.e. no long-distance forces, which would manifest from integrating the $\vec{a} \cdot \nabla_v$ term in the Boltzmann equation). The above equations require a closure relationship and equation of state; if one is supplied, then the above equations can be solved for $\rho, \vec{U}$, and e to obtain a macroscopic description of the hydrodynamic state.

To summarize, the origin of the hydrodynamics/fluid equations or the transport/radiation equation is the Boltzmann equation with a quadratic or linear collision functional, respectively.

- For radiation, the linearity of the scattering kernel causes the asymptotic (short mean free path) behavior to be described by a diffusion equation.
- For the fluid, the quadratic scattering kernel, along with the Chapman-Enskog equilibrium restriction, causes the asymptotic (short two-body mean free path) behavior to be described by the hydrodynamics equations.
- The difference in the scattering kernel implies different algorithmic requirements, but the asymptotic limit of either version of the Boltzmann equation permits optimization of the solution procedure in high-scattering regions (e.g. DDMC).

The opacities, which mediate the interaction of radiation with a material, must set the degree to which massive particles are accelerated, and hence must manifest as source terms in the Euler equations. Equivalently, these terms introduce emissivity (a source) into the transport equation. The resulting system of equations is nonlinear, even when the material is static. In the next section we develop the Langrangian form of the RH equations.

Development of the Lagrangian Radiation Hydrodynamics Equations

In conservative form, the inviscid Euler equations with external sources are similar to those shown in equation (11),

$$\frac{\partial \rho}{\partial t} + \nabla \cdot \left(\rho \vec{U}\right) = 0,$$
$$\frac{\partial \left(\rho \vec{U}\right)}{\partial t} + \nabla \cdot \left(\mathrm{P} + \rho \vec{U}\vec{U}\right) = \frac{1}{c}\vec{q},$$
$$\frac{\partial (\rho \mathcal{E})}{\partial t} + \nabla \cdot \left(\vec{U}(\rho \mathcal{E} + \mathrm{P})\right) = q_0 + \frac{\vec{U}}{c} \cdot \vec{q},$$

where $\vec{q}$ and q_0 are the external source terms, and $\mathcal{E} = e + U^2/2$. Differing from the previous section, the heat conduction flux term has been dropped, and the pressure tenser has been assumed to have no shear terms, so $\mathrm{P} = P\mathbf{I}$, where $\mathbf{I}$ is the identity tensor. Using the Lagrangian time derivative,

$$\frac{D}{Dt} = \frac{\partial}{\partial t} + \vec{U} \cdot \nabla,$$

the above equations can be cast in the Lagrangian form,

$$\begin{aligned} \frac{D\rho}{Dt} + \rho \nabla \cdot \vec{U} &= 0, \\ \rho \frac{D\vec{U}}{Dt} + \nabla \mathrm{P} &= \frac{1}{c}\vec{q}, \\ \rho \frac{De}{Dt} + P \nabla \cdot \vec{U} &= q_0. \end{aligned} \tag{12}$$

The second equation can be derived by utilizing the *Product Rule* on the derivatives in the momentum-conservation equation and eliminating terms that form the mass-conservation equation. Likewise, the third equation can be obtained by the Product Rule and eliminating terms that form the mass-conservation equation (multiplying e and $U = \left|\vec{U}\right|$) and substituting $\vec{q}/c$ for the terms dotting $\vec{U}$ that form the left side of the momentum-conservation equation. It is worth noting that the change from $q_0 + \vec{U} \cdot \vec{q}/c$ to q_0 in the transformation of the energy-conservation equation is not of relativistic origin, despite its appearance; q_0 and $\vec{q}$ are defined in one inertial, or "lab," frame.

Assuming the equation of state is known for the material (for instance, the gamma-law $P \sim \rho e$), more information is needed for q_0 and $\vec{q}$ to close the system of equations. If q_0 and $\vec{q}$ are sources due to a radiation field, then the additional information is the transport equation (10).

Having been integrated over the space of all single-particle velocities, the Euler equations are lower-dimensional than the transport equation. This suggests that equivalently, integrals of the transport equation have to be taken over frequency and direction, to couple with hydrodynamics,

$$\frac{\partial E}{\partial t} + \nabla \cdot \vec{F} = \tilde{q}_0,$$
$$\frac{\partial \vec{F}}{\partial t} + c\nabla \cdot \mathbb{P} = \vec{\tilde{q}},$$

Where $\tilde{q}_0$ and $\vec{\tilde{q}}$ follow from the transport equation. Assuming the total available momentum and energy is in either the fluid or the radiation field,

$$\tilde{q}_0 = -q_0,$$
$$\vec{\tilde{q}} = -\vec{q}.$$

Radiative transfer methods can calculate the energy and momentum absorbed into the material from the radiation can be tallied, which in turn permits calculation of q_0 and $\vec{q}$.

Material Motion Corrections

The question remains as to how to treat relativistic corrections. In Monte Carlo, Lorentz transformations to energy, frequency, and direction can be performed for each particle to boost into and out of the comoving frame of the fluid. While not discussed here, references [28, 24, 29, 30] provide full details of this treatment. Additional discussion of momentum deposition and material motion corrections are provided in the Jayenne physics manual [21]. Following this derivation, we arrive at the static-material transport equation with two extra terms for sub-relativistic regimes ($|\vec{U}|/c \ll 1$).

For reference, this moving materials photon transport equation is provided here along with the associated material energy balance equation that is required to close the system.

$$\frac{1}{c}\frac{\partial I}{\partial t} + \nabla \cdot \left(\frac{4}{3c}\vec{U}I\right) + \hat{\Omega} \cdot \nabla I + (\sigma_s + \sigma_a)I = \int_{4\pi}\int_0^\infty \sigma_s(\nu' \to \nu, \hat{\Omega}' \to \hat{\Omega})I' d\nu' \hat{\Omega}' + \sigma_a B - \frac{\vec{U}}{c} \cdot \frac{\vec{q}}{4\pi}, \tag{13}$$

$$\rho \frac{\partial e}{\partial t} = -q_0. \tag{14}$$

The radiation-hydrodynamic coupling terms q_0 and $\vec{q}$ are defined by x-ray emission from the material and x-ray absorption into the material. It is straightforward to show through limit analysis that

$$q_0 = \int_{4\pi}\int_0^\infty \sigma_a(B - I)d\nu' d\hat{\Omega}', \tag{15}$$

$$\vec{q} = \int_{4\pi}\int_0^\infty \sigma_t \hat{\Omega} I d\nu' d\hat{\Omega}' = \sigma_t \vec{F}. \tag{16}$$

Substituting the q_0 source expression into the material energy balance equation we arrive at

$$\rho \frac{\partial e}{\partial t} = c_v \frac{\partial T}{\partial t} = \int_{4\pi} \int_0^\infty \sigma_a (I - B) dv' d\hat{\Omega}'. \tag{17}$$

Before introducing the IMC linearization in the next session, we make a few additional modifications to the TRT equations. We begin by replacing the Planck function in equation (13) with the definitions provided in (4) and (7) and we replace the integral of the Planck function multiplied by the opacity in equation (17) using equation (8),

$$\begin{aligned} &\frac{1}{c}\frac{\partial I}{\partial t} + \nabla \cdot \left(\frac{4}{3c}\vec{U} I\right) + \hat{\Omega} \cdot \nabla I + (\sigma_s + \sigma_a) I \\ &\qquad = \int_{4\pi} \int_0^\infty \sigma_s (\nu' \to \nu, \hat{\Omega}' \to \hat{\Omega}) I' dv' d\hat{\Omega}' + \frac{\sigma_a c a T^4}{4\pi} - \frac{\vec{U}}{c} \cdot \frac{\vec{q}}{4\pi}, \end{aligned} \tag{18}$$

$$c_v \frac{\partial T}{\partial t} = \int_{4\pi} \int_0^\infty \sigma_a I dv' d\hat{\Omega}' - c a T^4 \sigma_P. \tag{19}$$

or, equivalently,

$$\frac{1}{\beta} \cdot \frac{\partial E}{\partial t} = \int_{4\pi} \int_0^\infty \sigma_a I dv' d\hat{\Omega}' - c a T^4 \sigma_P. \tag{20}$$

The IMC linearization

The Jayenne software package solves the system defined by linearizing equations (18) and (20) according the standard IMC method described in [31, 32]. A brief review of this linearization is provided next. The linearization process begins by discretizing the TRT equations over a time step using a fully implicit scheme in time,

$$\begin{aligned} &\frac{1}{c}\frac{I_{n+1} - I_n}{\Delta t} + \nabla \cdot \left(\frac{4}{3c}\vec{U}_n I_{n+1}\right) + \hat{\Omega} \cdot \nabla I_{n+1} + \left(\sigma_{s,n+1} + \sigma_{a,n+1}\right) I_{n+1} \\ &\qquad = \int_{4\pi} \int_0^\infty \sigma_{s,n+1} (\nu' \to \nu, \hat{\Omega}' \to \hat{\Omega}) I'_{n+1} dv' d\hat{\Omega}' + \frac{\sigma_{a,n+1} c E_{n+1}}{4\pi} - \frac{\vec{U}_n}{c} \cdot \frac{\vec{q}_n}{4\pi}, \end{aligned} \tag{21}$$

$$\frac{\mathcal{E}_{n+1} - \mathcal{E}_n}{\Delta t} = \int_{4\pi} \int_0^\infty \sigma_{a,n} I_{n+1} dv' d\hat{\Omega}' - c \sigma_{P,n} E_{n+1}, \tag{22}$$

and, *not equivalently*, we have via the IMC approximation,

$$\frac{1}{\beta_n}\frac{E_{n+1} - E_n}{\Delta t} = \int_{4\pi} \int_0^\infty \sigma_{a,n} I_{n+1} dv' d\hat{\Omega}' - c \sigma_{P,n} E_{n+1}. \tag{23}$$

Manipulating this material energy balance equation and solving for the end-of-timestep value for the radiation energy density, we have

$$E_{n+1} = \left(\frac{1}{1 + c\sigma_{P,n}\beta_n\Delta t}\right)E_n + \left(\frac{\beta_n\Delta t}{1 + c\sigma_{P,n}\beta_n\Delta t}\right)\int_{4\pi}\int_0^\infty \sigma_{a,n}I'_{n+1}dv'd\hat{\Omega}'.$$

This leads us to define a convenience parameter, the Fleck factor f_n,

$$f_n = \frac{1}{1 + \beta_n c\Delta t\sigma_{P,n}} = \frac{1}{1 + \frac{4aT_n^3 c\Delta t\sigma_{P,n}}{c_{v,n}}}, \qquad 1 - f_n = \frac{\beta_n c\Delta t\sigma_{P,n}}{1 + \beta_n c\Delta t\sigma_{P,n}}, \tag{24}$$

so that we have

$$E_{n+1} = f_n E_n + \frac{1}{c\sigma_{P,n}}\int_{4\pi}\int_0^\infty (1 - f_n)\sigma_{a,n}I'_{n+1}dv'd\hat{\Omega}'. \tag{25}$$

Inserting expression (25) into the temporally discretized TRT equation (21) and the material energy balance equation (22), we find

$$\begin{aligned}\frac{1}{c}\frac{I_{n+1} - I_n}{\Delta t} + \nabla\cdot\left(\frac{4}{3c}\vec{U}I_n\right) + \hat{\Omega}\cdot\nabla I_* + \left(\sigma_{s,n} + \sigma_{a,n}\right)I_* \\ = \int_{4\pi}\int_0^\infty \sigma_{s,n}\left(v' \to v, \hat{\Omega}' \to \hat{\Omega}\right)I'_* dv'd\hat{\Omega}' + f_n\sigma_{a,n}b_*\frac{cE_n}{4\pi} \\ + (1 - f_n)\frac{\sigma_{a,n}b_*}{\sigma_{P,n}}\frac{1}{4\pi}\int_{4\pi}\int_0^\infty \sigma_{a,n}I'_* dv'd\hat{\Omega}' - \frac{\vec{U}}{c}\cdot\frac{\vec{q}_n}{4\pi},\end{aligned} \tag{26}$$

$$\mathcal{E}_{n+1} = \mathcal{E}_n + \Delta t\int_{4\pi}\int_0^\infty f_n\sigma_{a,n}I_* dv'd\hat{\Omega}' - \Delta t f_n\sigma_{P,n}cE_n. \tag{27}$$

The above equations are the system solved by the Jayenne library. On the right hand side of equations (26) and (27), we have replaced the subscript $n+1$ with * to denote an arbitrary time centering evaluation that is used in practice. Once the end-of-timestep material energy is known, the material temperature, T_{n+1}, can be determined by inverting

$$\mathcal{E}_{n+1} = \mathcal{E}_n + \int_{T_n}^{T_{n+1}} c_v(T')dT'.$$

The following sections describe how this solution is coupled to the hydrodynamic solution from FLAG; first for IMC and then for the S_N solver.

IMC Algorithmic outline

The Jayenne library assumes the radiation transport will be operator-split from the hydrodynamics: during the Monte Carlo phase, the state of the material will be a snapshot. The operator split system is solved with sub-relativistic material motion corrections [29, 30] according to the following outline.

1. Solve the uncoupled hydrodynamic step in FLAG:
   These equations are the discretized-in-time form of equations (12). In all of the following equations the subscript *n* is the time step index, *h* denotes the value at the end of the pure hydrodynamic step, and [*] denotes an arbitrary time-centering evaluation.

$$\frac{\rho_{n+1}-\rho_n}{\Delta t}+\left[\nabla\cdot\left(\rho\vec{U}\right)\right]_*=0, \tag{28}$$

$$\frac{\rho_{n+1}\vec{U}_h-\rho_n\vec{U}_n}{\Delta t}+\left[\nabla\cdot\left(\rho\vec{U}\vec{U}\right)+\nabla P\right]_*=0, \tag{29}$$

$$\frac{\rho_{n+1}\mathcal{E}_h-\rho_n\mathcal{E}_n}{\Delta t}+\left[\nabla\cdot\left(\rho\mathcal{E}+P\right)\right]_*=0, \tag{30}$$

2. The next step is to solve radiation transport in Jayenne using the updated hydrodynamic state, *h*. There are thee substeps for the *O(v/c)* radiation transport algorithm.

   a. First, the initial census particles are advected by $4\vec{U}_h/3$,

$$\frac{I_h-I_n}{\Delta t}+\nabla\cdot\left(\frac{4}{3}\vec{U}_h I_n\right)=0, \tag{31}$$

   b. Using updated values from equation (31) , proceed with the standard IMC method for non-moving materials. Note that it may be useful to replace radiation energy density, *E,* with aT^4 by employing equation (4).

$$\begin{aligned}\frac{I_r-I_h}{c\Delta t}+\hat{\Omega}\cdot\nabla I_*+\sigma_{t,h}I_* &= \int_{4\pi}\int_0^\infty \sigma_{s,h}I'_*dv'd\hat{\Omega}'+f_h\sigma_{a,h}b_h\frac{cE_h}{4\pi}\\ &+(1-f_h)\frac{\sigma_{a,h}b_h}{4\pi\sigma_{P,h}}\int_{4\pi}\int_0^\infty \sigma_{a,h}I'_*dv'd\hat{\Omega}'.\end{aligned} \tag{32}$$

   where the subscript *r* denotes the end of the Monte Carlo step, *f* is the Fleck factor from equation (24), σ_P is the Planck opacity, *b* is the frequency normalized Plank function and [*] continues to denotes an arbitrary time-centering evaluation.

c. The third part of the transport operator split involves post-processing the Monte Carlo particles by scaling their energy weights to account for work done by the radiation to the fluid.

$$\frac{I_{n+1} - I_r}{\Delta t} = -\left[\vec{U} \cdot \frac{\vec{q}}{4\pi}\right]_*. \tag{33}$$

3. Once the transport is done, the hydrodynamic state must be updated by using the Monte Carlo tallies to account for the energy and momentum deposition from equations (32) and (33),

$$\rho_{n+1} \frac{\vec{U}_{n+1} - \vec{U}_h}{\Delta t} = \left[\frac{\vec{q}}{c}\right]_*, \tag{34}$$

$$\rho_{n+1} \frac{e_{n+1} - e_h}{\Delta t} = f_h [q_0]_{a,*} + [q_0]_{s,*}, \tag{35}$$

$$\rho_{n+1} \frac{U_{n+1}^2 - U_h^2}{2\Delta t} = \left[\frac{\vec{U}}{c} \cdot \vec{q}\right]_*, \tag{36}$$

where $[q_0]_{a,*}$ is the internal energy coupling due to absorption included in the IMC linearization and $[q_0]_{s,*}$ is the inelastic scattering coupling excluded from the IMC linearization. $\vec{U}_*$ is obtained by requiring consistency between equations (34) and(36), so

$$\vec{U}_* = \frac{1}{2}(\vec{U}_{n+1} + \vec{U}_h).$$

Since step 3 involves updating the fluid variables, it must be done by FLAG.

Full details concerning the calculation of momentum from step 2c (page 11) in this algorithm are provided in the Jayenne physics manual [21].

The above three step algorithm captures the RH operator split used by LUMOS. Step 2 is solved by the external TRT library, while the other two steps are solved by FLAG.

The S_N linearization

The Sn linearization is not fundamentally different from the IMC linearization, except in its linearization of the source term in the radiation step (step 2, above). Like the Jayenne library, the Capsaicin library assumes the radiation transport will be operator-split from the hydrodynamics: during the Sn transport phase, the state of the material will be a snapshot. The radiation solve step, which uses the updated hydrodynamic state, *h*, iteratively solves the linearized equations

$$\frac{I_r - I_h}{c\Delta t} + \hat{\Omega} \cdot \nabla I_r + \sigma_{t,h} I_r = \int_{4\pi} \int_0^\infty \sigma_{s,h} I_r' dv' d\hat{\Omega}' + \sigma_{a,h}\left(B_h + \frac{dB_h}{dx}(T_r - T_h)\right) \tag{37}$$

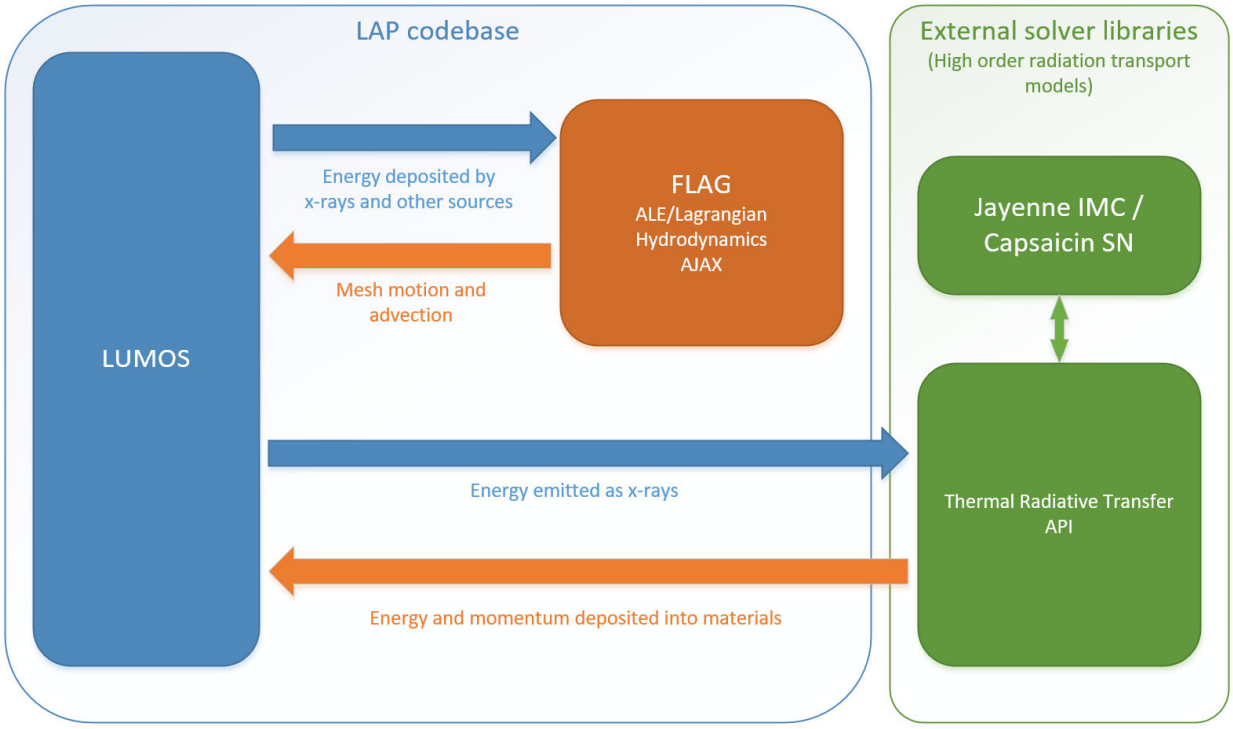

Figure 1. LUMOS code organization

S_N algorithm outline

The Sn algorithm follows essentially the same steps as the IMC, except that radiation momentum deposition (radiation forces) are calculated explicitly just prior to the hydrodynamics step, and the resulting radiation work is subtracted from the radiation field just prior to the radiation transport solve step.

Design Concept of LUMOS

The LUMOS code is designed so that the development of FLAG and the thermal radiative transfer solver libraries can be independent. Only the API layer needs careful and coordinated efforts between the three code efforts. The higher order x-ray transport solvers can be viewed as optional plug-and-play solver libraries. Each code contributes capabilities that are developed independently, but a light weight API allows these codes to be combined for multi-physics simulations.

Figure 1 above shows the organization of the LUMOS code. The LUMOS code is a superset of the hydrodynamics code FLAG. Both are built upon an object-oriented software layer called AJAX. AJAX provides a centralized, hierarchical, data-store for organizing simulation state based on class instances and a key-value lookup mechanism for accessing this data. AJAX also provides a flexible system of run-time

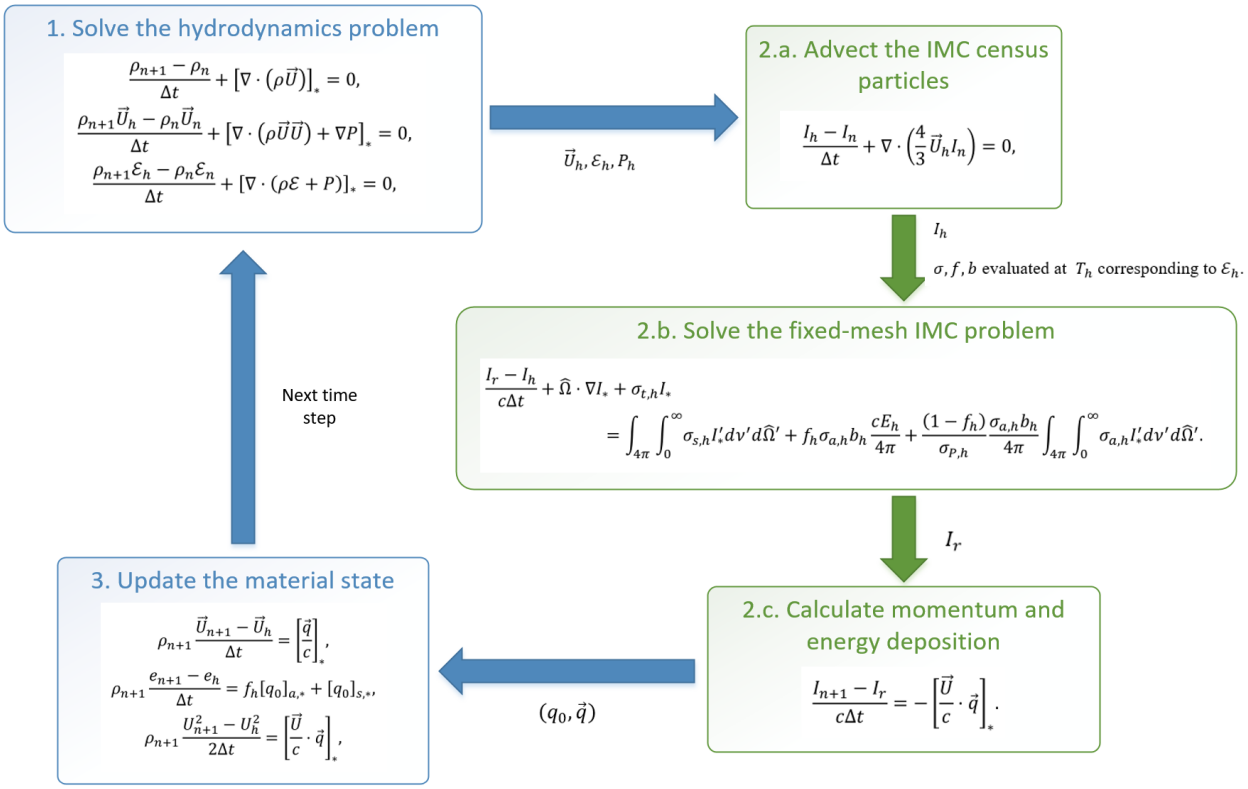

Figure 2. Pictorial representation of primary calculation phases for a single RH timestep. Each step represents an operator-split calculation. Green boxes represent the TRT solver and blue boxes represent the LAP codebase. The primary physics parameters handed to each step are listed next to the order-of-operation arrows.

polymorphism that allows modular components to easily connect and contribute updates to the simulation.

Within the AJAX system for LUMOS, an additional TRT module exists that interfaces with externally provided libraries that accurately model x-ray transport. The API routines are part of the LAP code and manipulate LAP data structures into a form acceptable for use by the TRT libraries. It should be noted that FLAG itself contains a gray diffusion radiation transport solver that does not require the TRT API. Only one of the high-order TRT libraries may be active at a time.

Both FLAG and LUMOS process physics solvers in a particular order specified by the selected operator split system of equations. As depicted in Figure 2, these calls to physics solvers are repeated for each time step until a stop condition is reached. For the LUMOS system the hydrodynamic solver is solved first followed by the radiation transport solver. Unlike many other RH solvers [5], LUMOS uses the same mesh for all portions of the calculation. This eliminates the need to map mesh and system state variables between two or more overlay meshes used by different physics solvers.

In this model, LUMOS retains full responsibility for

- reading input files/specifications, mesh, and material details,
- interfacing with libraries that provide physical data like opacities and Equation-of-State values that must be passed to the TRT solver libraries,
- managing energy balance,
- controlling the time step size,
- post processing of the solution,
- generation of restart dump files, and
- generation of visualization files.

This model allows LUMOS to remain in control of the core simulation and data and avoids contention of external resources by the TRT packages.

Mixed Materials and ALE

In full Lagrangian mode, there is no material mixing. However, to keep the mesh from tangling FLAG frequently employs an ALE step that introduces multiple materials in each computational cell. The TRT solver relies on FLAG to create new materials, one per cell. The current implementation is limited to using a simple atomic mix model to compute opacities and specific heats for a single material temperature per cell.

Acceleration algorithms for transport

In the current implementation, the unstructured mesh features of Jayenne's IMC solver are limited to Random Walk and optimized GPU transport kernels (if GPUs are available). Both of these acceleration techniques are internal to the IMC package and can be used without additional complication. For structured meshes, the Jayenne IMC solver recommends the use of Discrete Diffusion Monte Carlo, DDMC, but this is not currently available in LUMOS. Adding DDMC will reduce the computational cost of step 2.b., but it also makes step 2.c. more complicated [21].

Verification

To verify the correctness of this RH implementation, many standard tests have been run and the results reviewed by subject matter experts. While there are artifacts in some solutions due to known limitations of the existing implementation, the reviewers agreed that Lumos is performing correctly for a wide range of problems. Detailed reporting of these test problems and results are provided in [7, 33].

Conclusion

This memo has presented the mathematical/physics models and computer code structure used by the LUMOS code. This code couples the mature Lagrangian/ALE hydrodynamics of FLAG with the robust, high-order TRT solvers offered by the Jayenne and Capsaicin software projects by leveraging an operator-split methodology. The approach of this development is similar to that employed by SYMPHONY.

References

[1] D. E. Burton, "Connectivity structures and differencing techniques for staggered-grid free-lagrange hydrodynamics," Lawrence Livermore National Laboratory, Technical Report UCRL-JC-110555, Livermore, CA, 1992.

[2] D. E. Burton, "Consistent finite-volume discretization of hydrodynamic conservation laws for unstrucunstructured grids," Lawrence Livermore National Laboratory, Technical Report, Livermore, CA, 1994.

[3] J. Hill, "FLAG User's Manual," Los Alamos National Laboratory, Technical Report LA-CP-16-20334, Los Alamos, NM, 2017.

[4] "FY20 L2 Milestone (Demonstrate new x-ray transport code capability)," Los Alamos National Laboratory, ASC nWBS Subprogram IC, Los Alamos, NM, 2020.

[5] H. Park, "Radiation Hydrodynamics in the Ristra Project's Symphony code: Initial release," Los Alamos National Laboratory, Technical Report LA-UR-21-21267, Los Alamos, NM, 2021.

[6] M. Gittings, R. Weaver, M. Clover, T. Betlach, N. Byrne, R. Coker, E. Dendy, R. Hueckstaedt, K. New, W. R. Oakes, D. Ranta and R. Stefan, "The RAGE radiation-hydrodynamics code," *Computational Science & Discovery,* vol. 1, no. 1, 2008.

[7] R. T. Wollaeger, M. Cleveland, K. Thompson and N. Denissen, "Demonstration of a new unstructured mesh IMC x-ray transport capability in LAP codes," Los Alamos National Laboratory, Technical Report LA-UR-20-26697, Los Alamos, NM, 2020.

[8] E. Lefebvre, S. Bernard, C. Esnault, P. Gauthier, A. Grisollet, P. Hoch, L. Jacquet, G. Kluth, S. Laffite, S. Liberatore, I. Marmajou, P. Masson-Laborde, O. Morice and J.-L. Willien, "Development and validation of the TROLL radiation-hydrodynamics code for 3D hohlraum calculations," *Nuclear Fusion,* vol. 59, no. 3, 2019.

[9] T. Harries, T. J. Haworth, D. Acreman, A. Ali and T. Douglas, "The TORUS radiation transfer code," *Astronomy and Computing,* vol. 27, pp. 63-95, April 2019.

[10] L. Buntemeyer, R. Banerjee, T. Peters, M. Klassen and R. E. Pudritz, "Radiation hydrodynamics using characteristics on adaptive decomposed domains for massively parallel star formation simulations," *New Astronomy,* no. 43, pp. 49-69, 2016.

[11] A. Smith, R. Kannan, T. B. T.-H., M. Vogelsberger and R. Pakmor, "AREPO-MCRT: Monte Carlo Radiation Hydrodynamics on a Moving Mesh," *The Astrophysical Journal,* vol. 905, p. 27, 10 December 2020.

[12] B. R. Ryan, J. C. Dolence, Gammie and Charles, "bhlight: General Relativistic Radiation Magnetohydrodynamics with Monte Carlo Transport," *Astrophysical Journel,* vol. 807, no. 1, p. 31, 2015.

[13] R. Ramis and J. Meyer-ter-Vehn, "MULTI-IFE - A one-dimensional computer code for Inertial Fusion Energy (IFE) target simulations," *Computer Physics Communications,* vol. 203, pp. 226-237, 2016.

[14] R. Ramis, J. Meyer-ter-Vehn and J. Ramirez, "MULTI2D - A computer code for two-dimensional radiation hydrodynamics," *Computer Physics Communications,* vol. 180, no. 6, pp. 997-994, 2009.

[15] R. Ramis, R. Schmalz and J. Meyer-ter-Vehn, "Multi - A computer code for one-dimensional multigroup radiation hydrodynamics," *Computer Physics Communications,* vol. 49, no. 3, pp. 475-505, 1988.

[16] J. Honrubia, "A synthetically accelerated scheme for radiative transfer calculations," *Journal of Quantitative Spectroscopy and Radiative Transfer,* vol. 49, no. 5, pp. 491-515, May 1993.

[17] J. M. Stone, D. Mihalas and M. Norman, "ZEUS-2D: A Radiation Magnetohydrodynamics Code for Astrophysical Flows in Two Space Dimensions: III. The Radiation Hydrodynamic Algorithms and Tests," *The Astrophysical Journal Supplement Sieries,* vol. 80, no. 2, pp. 819-845, 1992.

[18] S. Davis, J. Stone and Y.-F. Jian, "A Radiation Transfer Solver for Athena Using Short Characteristics," *The Astrophysical Journal Supplement Series,* vol. 199(1), February 2012.

[19] J. Yan-Fie, J. M. Stone and S. W. Davis, "An Algorithm for Radiation Magnetohydrodynamics Based on Solving the Time-dependent Transfer Equation," *The Astrophysical Journal Supplement Series,* vol. 213, no. 1, p. 7, June 2014.

[20] E. Livne, A. Burrows, R. Walder, I. Lichtenstadt and T. A. Thompson, "Two-dimensional Time-dependent, Multigroup, Multiangle Radiation Hydrodynamics Test Simulation in the Core-Collapse Supernova Context," *The Astrophysical Journal,* vol. 609, no. 1, pp. 277-287, 2004.

[21] R. Wollaeger, M. Cleveland, K. Thompson, K. Long, A. Long and T. Kelley, "Jayenne Physics Manual, Version 8, An Implicit Monte Carlo Code for Thermal Radiative Transfer," Los Alamos National Laboratory, Los Alamos, NM, 2021 (unpublished).

[22] G. Habetler and B. Matkowsky, "Uniform asymptotic expansion in transport theory with small mean free paths and the diffusion approximation," *J. Math Phys.,* vol. 16, p. 846, 1975.

[23] P. T. Gressman and R. M. Strain, "Global classical solutions of the Boltzmann equation with long-range interactions," in *Proceedings of the National Academy of Science*, 2010.

[24] D. Mihalas and B. Mihalas, Foundations of Radiation Hydrodynamics, Oxford University Press, 1984.

[25] I. Sagert, W. Bauer, D. Colbry, J. Howell, R. Pickett, A. Staber and T. Strother, "Hydrodynamic shock wave studies within a kinetic monte carlo approach," *Journal of Computational Physics,* vol. 226, pp. 191-213, 2014.

[26] S. Chapman and T. Cowling, The mathematical theory of non-uniform gases: An account of the kinetic theory of visosity, thermal conduction and diffusion in gases., vol. 1, Cambridge University Press, 1970, pp. 27-52.

[27] H. Grad, "Asymptotic Theory of the Boltzmann Equation," *The Physics of Fluids,* vol. 6, pp. 147-181, 1963.

[28] J. Castor, Radiation Hydrodynamics, Cambridge University Press, 2004.

[29] R. Lowrie and A. Wollaber, "Simple material-motion corrections for thermal radiative transport," *Journal of Computational and Theoretical Transport,* vol. 43, pp. 148-161, 2014.

[30] A. Wollaber, H. Park, R. Lowrie, R. Rauenzahn and M. Cleveland, "Rad-Hydro with a High-Order, Low-Order Method," Los Alamos National Laboratory, Technical Report LA-UR-15-26171, Los Alamos, NM, 2015.

[31] J. Fleck and J. Cummings, "An implicit Monte Carlo scheme for calculating time and frequency dependent nonlinear radiation transport," *Journal of Computational Physics,* vol. 8, pp. 313-342, 1971.

[32] A. Wollaber, "Four Decades of Implicit Monte Carlo," *Journal of Computational and Theoretical Transport,* pp. 1-70, 2016.

[33] R. Wollaeger, K. Budge, N. Denissen, K. Thompson, M. Cleveland, A. Till and J. Chang, "L3 Milestone Report," Los Alamos, NM 87545, 2021.

[34] K. Thompson, M. L. A. R. Cleveland, R. Wollaeger and K. Long, "Release of Jayenne-8.0.0, Revision 2," Los Alamos National Laboratory, Technical Report CCS-2:19-009(U), Los Alamos, NM, 2019.

[35] T. Evans and J. Densmore, "Methods for coupling radiation, ion, and electron energies in grey Implicit Monte Carlo," *Journal of Computational Physics,* vol. 225, pp. 1695-1720, 2007.

Distribution

CCS-2 Group Office	ccs2go@lanl.gov	CCS-2	MS D413
Alex Long	along@lanl.gov	CCS-2	MS D409
Andrew Till	till@lanl.gov	CCS-2	MS D409
Ben Ryan	brryan@lanl.gov	CCS-2	MS D413
David Dixon	ddixon@lanl.gov	CCS-2	MS D409
Edward Norris	enorris@lanl.gov	XCP-1	MS T086
Jae Chang	jhchang@lanl.gov	CCS-2	MS D409
Jeff Haack	haack@lanl.gov	CCS-2	MS D409
Jim Warsa	warsa@lanl.gov	CCS-2	MS D409
Jimmy Fung	fung@lanl.gov	XCP-DO	MS T086
Joe Zerr	rzerr@lanl.gov	CCS-2	MS D409
Jon Dahl	dahl@lanl.gov	CCS-2	MS D409
Kendra Long	keadyk@lanl.gov	CCS-2	MS B256
Kent Budge	kgbudge@lanl.gov	CCS-2	MS D409
Markus Berndt	berndt@lanl.gov	CCS-2	MS D413
Matt Cleveland	cleveland@lanl.gov	CCS-2	MS D409
Rob Lowrie	lowrie@lanl.gov	CCS-2	MS D413
Ryan Wollaeger	wollaeger@lanl.gov	CCS-2	MS D409
Wes Even	even@lanl.gov	CCS-2	MS D413